Numerical Approximation of the One-dimensional Inverse Stefan Problem Using a Meshless Method

Mohammed Baati, Nada Chakhim, Mohamed Louzar and Abdellah Lamnii

***Abstract*—This paper employs a recent algorithm capable of determining an optimal regularization technique based on a meshless method of fundamental solutions for the one-dimensional inverse Stefan problem, where the boundary data is reconstructed on the fixed boundary. The inverse problem is ill-posed. For comparison purposes, we employ Tikhonov, Truncated Singular Value Decomposition, and Randomized Singular Value Decomposition regularization methods to obtain a more accurate solution. The numerical results of three different benchmark examples are presented in this paper.**

***Index Terms*—inverse problem, problem the Stefan, tikhonov, truncated singular value decomposition, randomized singular value decomposition, method of fundamental solutions.**

I. Introduction

THE Stefan problem model arises in various real-world and engineering situations involving melting or freezing that cause a boundary to change over time [1]. Examples include the solidification of metals, melting, casting, crystal growth, freezing of water and food, ablation, and more. The direct Stefan problem allows us to determine both the temperature and the moving boundary interface when provided with initial and boundary conditions, as well as the thermal properties of the heat-conducting body.

In contrast, the primary goal of the inverse Stefan problem is to determine the initial condition, boundary condition, and thermal properties from complementary information. This may involve partial knowledge or measurements of the moving boundary interface location, its velocity in a normal direction, and the temperature at the selected interior thermocouples within the domain [2], [3]. Furthermore, the inverse Stefan problem belongs to a significant class of ill-posed control theory problems with numerous engineering applications.

For instance, in the material refining technology that utilizes recrystallization, solving the inverse Stefan problem becomes crucial. It involves finding the temperature and heat flux at the fixed surface to ensure the flatness of the crystallization front.

Solutions to both the direct and inverse Stefan problems often pose challenges for popular numerical methods like the Finite Element Method (FEM) [4] and the Finite Difference Method (FDM) [5], [6]. This difficulty arises due to the free boundary changing in the domain mesh at each time instant for these methods. To address this issue, the Boundary Element Method (BEM) [7] partially mitigates the problem by only discretizing the boundary of the solution domain.

However, a more efficient and simplified approach with easier computational implementation is offered by the Method of Fundamental Solutions (MFS). MFS eliminates the need for domain mesh and requires only suitable placement of collocation points on the initial base/boundary of the solution domain, along with source points located external to this boundary. In this study, we will investigate how the location of these source points affects the accuracy of the approximate solution.

Recently, the fundamental solutions method has been successfully applied to various hyperbolic and parabolic problems, including direct and inverse Stefan problems. The simplicity of the technique and the ease with which it can be implemented have made it widely known.

For the advantages of MFS over other more traditional methods of domain or boundary discretization, references [8] and [9] can be consulted. In this study, we have developed the Method of Fundamental Solutions (MFS) based on the Randomized Singular Value Decomposition (rSVD). Several rSVD inversion algorithms have been proposed [10], [11]. rSVD leverages the intrinsic low-rank structure of inversion problems to construct an accurate approximation efficiently.

Our main contribution lies in providing a framework for developing the fundamental solutions method based on rSVD and demonstrating the robustness of this approach. To facilitate comparison, we will evaluate this method against two widely recognized regularization techniques: Truncated Singular Value Decomposition (TSVD) and Tikhonov regularization [2].

The outline of this paper is organized as follows: In Section 2, we will formulate the inverse Stefan problem and discuss some of its variants. In Section 3, we present the Method of Fundamental Solutions (MFS) for solving the inverse Stefan problem numerically and provide a recap of its theoretical properties. In Section 4, we introduce various regularization methods. Section 5 will showcase numerical results demonstrating that an accurate approximation of the inverse Stefan problem can be achieved using MFS with rSVD regularization.

II. Mathematical formulation

In the direct one-dimensional Stefan problem, we aim to determine the free boundary which we denote by R_M and is given by x=M(t) and the temperature solution v(x,t) in the heat conduction domain Ω=(0,M(t))$\times$(0,t_f], when $t_f>0$ is the fixed boundary at x=0, which we call by R_v. We denote the union of the boundaries by R=$R_M \cup R_v$ and the closure of the domain Ω by $\bar{\Omega}$=[0,M(t)]$\times$[0,t_f].

In the direct one-phase Stefan problem we aim to determine the solution v(x,t) as well as the moving boundary given

Manuscript received February 9, 2023; revised November 3, 2023.

Mohammed BAATI is a PhD student at Hassan First University of Settat, FST, MISI Lab, Settat, Morocco (e-mail: m.baati@uhp.ac.ma)

Nada Chakhim is a Doctor at Hassan First University of Settat, FST, MISI Lab, Settat, Morocco (e-mail: nada.chakhim@gmail.com)

Mohamed Louzar is a professor at Hassan First University of Settat, FST, MISI Lab, Settat, Morocco (e-mail: mohamed.louzar@uhp.ac.ma)

Abdellah Lamnii is a professor at Abdelmalek Essaadi University, LaSAD, ENS, 93030, Tetouan, Morocco (e-mail: a.lamnii@uae.ac.ma)

by x=M(t), satisfying the heat equation

$$\frac{\partial v}{\partial t}(x,t) - \frac{\partial^2 v}{\partial x^2}(x,t) = 0, (x,t) \in \Omega \quad (1)$$

Subject to the initial condition

$$v(x,0) = v_0(x), x \in [0,b], M(0) = b > 0 \quad (2)$$

Where $v_0 \in C^1([0, M(0)])$.

The Dirichlet and Neumann boundary conditions on the moving boundary x=M(t)

$$v(M(t),t) = 0, t \in (0, t_f] \quad (3)$$

$$\frac{\partial v}{\partial x}(M(t),t) = -M'(t), t \in (0, t_f] \quad (4)$$

With $M \in C^1([0,t_f])$ is a positive function.

We have Dirichlet and Neumann boundary conditions at the fixed boundary x=0

$$v(0,t) = h(t), t \in (0, t_f] \quad (5)$$

$$-\frac{\partial v}{\partial x}(0,t) = g(t), t \in (0, t_f] \quad (6)$$

The existence and uniqueness of a solution, along with its continuous dependence on the data, have been established and can be found in references [12] and [13].

The boundary conditions given by equations (3) and (4) can be replaced by the general boundary conditions given by

$$v(M(t),t) = h_1(t), t \in (0, t_f] \quad (7)$$

$$\frac{\partial v}{\partial x}(M(t),t) = h_2(t), t \in (0, t_f] \quad (8)$$

Where h_1, $h_2 \in C^1([0,t_f])$ which satisfy the compatibility conditions $h_1(0) = v_0(M(0))$ and $h_2(0) = v_0'(M(0))$.

The inverse Stefan problem considered in this study involves finding the temperature v(x,t) that satisfies equations (1)-(4), with M(t) known. A simple approach proposed in [2] uses the Method of Fundamental Solutions with Tikhonov regularization. However, in our research, we employ the Method of Fundamental Solutions with rSVD regularization to tackle the ill-posed nature of the problem and enhance convergence.

III. The Method of Fundamental Solutions (MFS)

We refer to the fundamental solutions of the one-dimensional heat equation (1) as presented in references [14] and [15].

$$E(x,t,y,\mu) = \frac{H(t-\mu)}{(4\pi(t-\mu))^{\frac{1}{2}}} e^{\frac{-(x-y)^2}{4(t-\mu)}} \quad (9)$$

Where H is the Heaviside function.

We construct a novel version of the method of fundamental solutions to approximate equations (1)-(4) using a linear combination of the fundamental solutions provided by:

$$v_\infty(x,t) = \sum_{j=1}^{2} \sum_{n=1}^{\infty} c_n^{(j)} E(x,t,y_j(\mu_n),\mu_n), (x,t) \in \bar{\Omega} \quad (10)$$

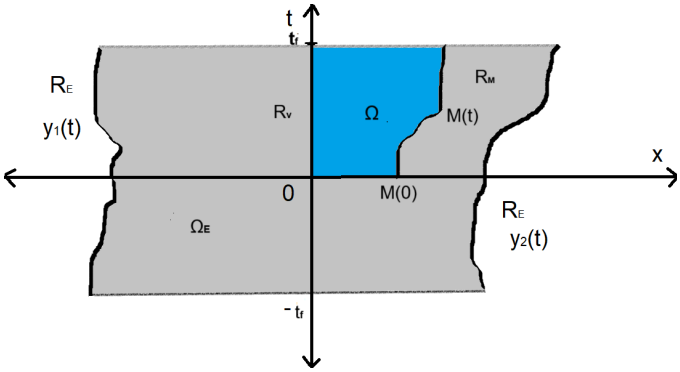

Fig. 1. General representation of the domain Ω, boundary $R = R_v \cup R_M$, and source points placed on R_E external to the domain Ω.

To implement the Method of Fundamental Solutions for the inverse Stefan problem, we truncate equation (10) by considering a finite number of terms, specifically,

$$v_N(x,t) = \sum_{j=1}^{2} \sum_{n=1}^{2N} c_n^{(j)} E(x,t,y_j(\mu_n),\mu_n), (x,t) \in \bar{\Omega} \quad (11)$$

We construct a one-dimensional domain with a fixed boundary at x=0 and a moving boundary at x=M(t). Source points are positioned at the following coordinates:

$$(-l, \mu), \mu \in (-t_f, t_f)$$

$$(l + M(\mu), \mu), \mu \in (0, t_f)$$

$$(l + M(-\mu), \mu), \mu \in (-t_f, 0)$$

Source points have been located symmetrically concerning μ via a reflection through t=0. We will test other source point locations to improve the results.

The source points will be set to time points $(\mu_n)_{n=1,\ldots,2N} \in (-t_f, t_f)$ given by

$$\mu_n = \frac{2(n-N)-1}{2N} t_f, n = 1, ..., 2N$$

$$y_1(\mu_n) = -l, n = 1, ..., 2N$$

$$y_2(\mu_n) = l + M(|\mu_n|), n = 1, ..., 2N$$

We have in total 4N source points on the boundary R_E, and we place the same number of collocation points on the lateral and base surfaces $M_0 \cup R_v$. We note that the location of the collocation points may be arbitrary, but in what follows we set them uniformly for ease of implementation. Let

$$t_i = \frac{i}{N} t_f, x_1^{(i)} = M(t_i), i = 0, ..., N$$

$$x_0^{(k)} = \frac{kM(0)}{K+1}, k = 1, ..., K$$

We get the following equation system:

$$v_N(x_0^{(k)}, 0) = v_0(x_0^{(k)}), k = 1, ..., K \quad (12)$$

$$v_N(x_1^{(i)}, t_i) = 0, i = 0, ..., N \quad (13)$$

$$\frac{\partial v_N}{\partial x}(x_1^{(i)}, t_i) = -M'(t_i), i = 0, ..., N \quad (14)$$

The system of equations (12)-(14) contains k+2(N+1) equations and 4N unknowns. Therefore, we get k≥2N-2 [12], [13], which is a necessary condition for a unique solution. This system can be represented as follows

$$Ac = g \tag{15}$$

Where c represents the vector of unknown constants $c_n^{(j)}$, g is the vector describing the initial and boundary values at the collocation points, and A is the matrix representing the value of the fundamental solutions at the corresponding collocation and source points.

Matrix A has a high condition number [16], [17], which necessitates the application of regularization methods, such as Tikhonov regularization [18], randomized singular value decomposition, and truncated singular value decomposition, to achieve better regularization.

IV. Regularization methods

The solution to the ill-conditioned linear system requires special treatment using regularization methods. Notably, the Tikhonov regularization method stands out as one of the oldest and most widely used approaches. In its simplest form, the Tikhonov regularization replaces the linear system (15) with the following regularized system

$$(A^{tr}A + \alpha I)c = A^{tr}g \tag{16}$$

Where α is a regularization parameter that determines the quality of the approximate solution and I is a unit matrix. The choice of the regularization parameter $\alpha \geq 0$ is chosen according to the L-curve criterion see [19]. We can apply the truncated singular value decomposition (TSVD) method, which is one of the most powerful tools in numerical linear algebra [20].

For the matrix A$\in R^{n\times n}$ the SVD of A is defined by

$$A = U\sum V^{t_f} = \sum_{i=1}^{n} u_i\sigma_i v_i^{t_f}$$

Where U=$(u_1, u_2, u_3, ..., u_n)$, V=$(v_1, v_2, v_3, ..., v_n)$ are orthonormal column matrices with size n×n. $\Sigma=\begin{pmatrix} D & 0 \\ 0 & 0 \end{pmatrix}$, which D=diag$(\sigma_1, \sigma_2, ..., \sigma_n)$, and σ_i is the singular value of A and satisfies $\sigma_1 > \sigma_2 > ... > \sigma_n$. When singular values in the matrix are very small, the condition number of the matrix A becomes very large. To mitigate this issue, the best approach is to reduce the condition number of A by truncating the very small singular values using the TSVD method.

The truncated SVD (TSVD) approximation of A as a matrix A_k such as

$$A_k = U\sum_k V^{t_f} = \sum_{i=1}^{k} u_i\sigma_i v_i^{t_f}$$

With $\Sigma_k = diag(\sigma_1, \sigma_2, ..., \sigma_k, 0, ..., 0) \in R^{n\times n}, k \leq n$ where $\sum_k$ equals $\sum$ with the smallest n-k singular values replaced by zeros. u_i and v_i are the columns of the matrices U and V, respectively. The TSVD solution to (15) is defined by:

$$c_k = A_k^{-1}g = \sum_{i=1}^{k} \frac{u_i^{t_f} g}{\sigma_i} v_i$$

The theory of random singular value decomposition (rSVD) is employed to extract the principal information from the convolution [21]. The main goal of this method is to compute a q-rank approximation of the matrix A with q≪n.

$$\tilde{A}_q = \tilde{U}\tilde{\sum}V^{\tilde{t}_f}$$

Where the U and V are orthogonal unitary matrices with size n×q. $\tilde{U}=(\tilde{u_1}, \tilde{u_2}, ..., \tilde{u_q})$ and $\tilde{V}=(\tilde{v_1}, \tilde{v_2}, ..., \tilde{v_q})$ are both orthonormal, and $\tilde{\sum}$ is a diagonal matrix with nonzero diagonal entries $\tilde{\sigma_1}$ through $\tilde{\sigma_q}$, with $\tilde{\sigma_1} > \tilde{\sigma_2} > \tilde{\sigma_3} > ... > \tilde{\sigma_q} > 0$. The diagonal entries $\tilde{\Sigma}$ of the approximate singular value of the A.

The steps of the rSVD method are [22]:

- Form an n×q Gaussian random matrix Ω.
- Construct a matrix Y=AΩ.
- Decomposition of Y.(Y=$Q_y R_y$, such that R_y is the upper triangular matrix).
- Construct the q×n approximate matrix C=$A^{t_f} Q_y$.
- Decomposition QR: C=$Q_c R_c$.
- Determine the SVD: $R_c = U_c \Sigma_c V_c^{t_f}$ where $\Sigma = \Sigma_c$.
- Construct the matrix U =$Q_y V_c$, $V^{t_f} = U_c^{t_f} Q_c^{t_f}$.

The well-conditioned linear system can be solved using any classical method such as the Gaussian elimination method for example [23].

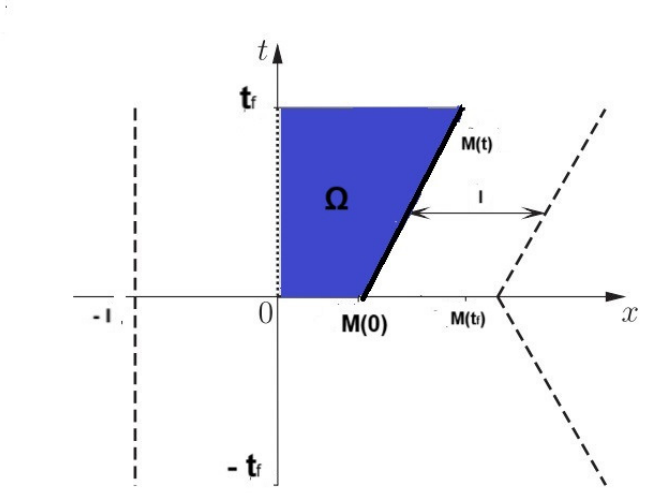

Fig. 2. Particularization of Fig. 1 for three examples.

V. Numerical results

This section presents some numerical tests to demonstrate the performance of the Method of Fundamental Solutions with rSVD regularization. We will use this method to approximate two examples.

A. Example 1

The first example has a moving boundary given by the function

$$M(t) = \sqrt{2} - 1 + \frac{t}{\sqrt{2}}, t \in [0, 1] \tag{17}$$

The source points are located on the external boundaries $(-l, \mu), \mu \in (-1, 1), (M(\mu)+l, \mu), \mu \in (0, 1), (M(-\mu)+l, \mu), \mu \in (-1, 0)$.

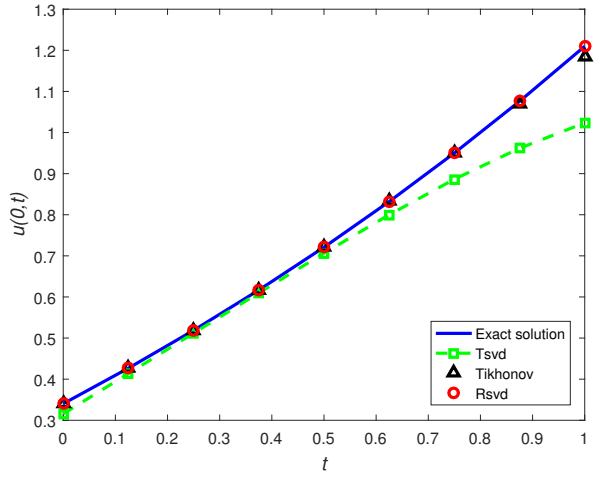

Fig. 3. The comparison of the exact solution and the MFS approximation using three methods generated by l=2.5, $\alpha = 10^{-6}$, k=30 and N=16.

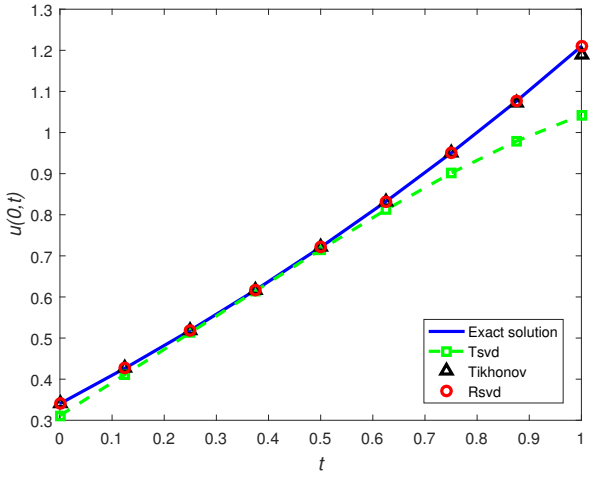

Fig. 4. The comparison of the exact solution and the MFS approximation using three methods generated by l=2.5, $\alpha = 10^{-6}$, k=30 and N=32.

TABLE I
THE SIMULATION CONDITIONS.

Hardware or Software	Parameters
CPU	Intel(R) Core (TM) i7-10750H CPU
RAM	16 Go
Platform	MATLAB R2016a

The exact solution is given by

$$v(x,t) = -1+\exp(1-\frac{1}{\sqrt{2}}+\frac{t}{2}-\frac{x}{\sqrt{2}}), (x,t) \in [0, M(t)]\times[0,1] \tag{18}$$

with the following initial and boundary conditions

$$v(x,0) = -1+\exp(1-\frac{1}{\sqrt{2}}-\frac{x}{\sqrt{2}}), x \in [0, M(0)], M(0) = \sqrt{2}- \tag{19}$$

$$v(M(t),t) = 0, t \in (0,1] \tag{20}$$

$$\frac{\partial v}{\partial x}(M(t),t) = -M'(t) = -\frac{1}{\sqrt{2}}, t \in (0,1] \tag{21}$$

The Dirichlet boundary and Neumann conditions on the fixed boundary x=0 is given by

$$v(0,t) = -1 + \exp(1 - \frac{1}{\sqrt{2}} + \frac{t}{2}), t \in (0,1] \tag{22}$$

$$\frac{\partial v}{\partial x}(0,t) = -\frac{1}{\sqrt{2}} \exp(1 - \frac{1}{\sqrt{2}} + \frac{t}{2}), t \in (0,1] \tag{23}$$

We will choose α=10^{-6} of the L-curve for the regularization parameter [25]. The simulation conditions are given in Table 1.

We will choose a new value α=10^{-5} of the L-curve for the regularization parameter [25].

In this example, our objective is to determine the Neumann boundary conditions along the fixed boundary x=0. In Figures 3-6, we present the MFS approximations for v(0,t) using three regularization methods: Tikhonov, TSVD, and rSVD with α=10^{-6}. Upon comparison, all methods show good correspondence with the exact solution. However, as the number of source points increases, the accuracy notably improves for the rSVD regularization method compared to the Tikhonov and TSVD methods.

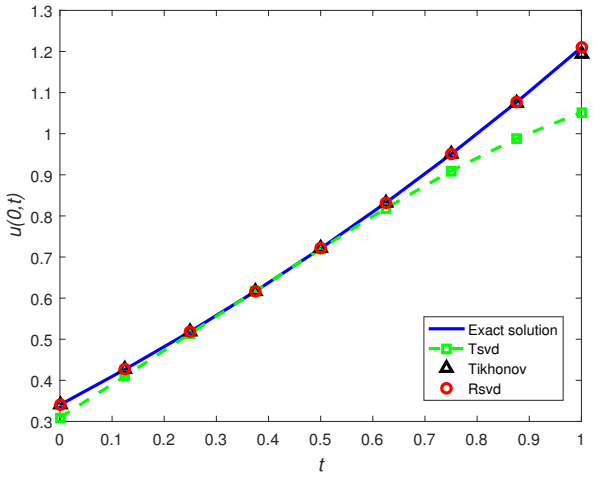

Fig. 5. The comparison of the exact solution and the MFS approximation using three methods generated by l=2.5, $\alpha = 10^{-6}$, k=30 and N=64.

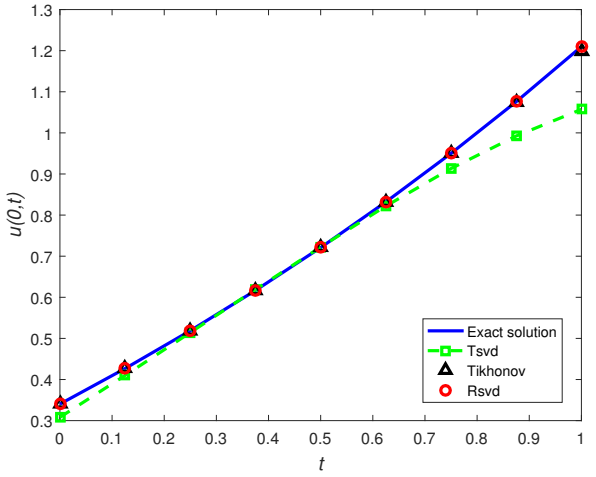

Fig. 6. The comparison of the exact solution and the MFS approximation using three methods generated by l=2.5, $\alpha = 10^{-6}$, k=30 and N=128.

Figures 11-14 also show that, as expected, the heat flux can be accurately estimated by the rSVD method compared

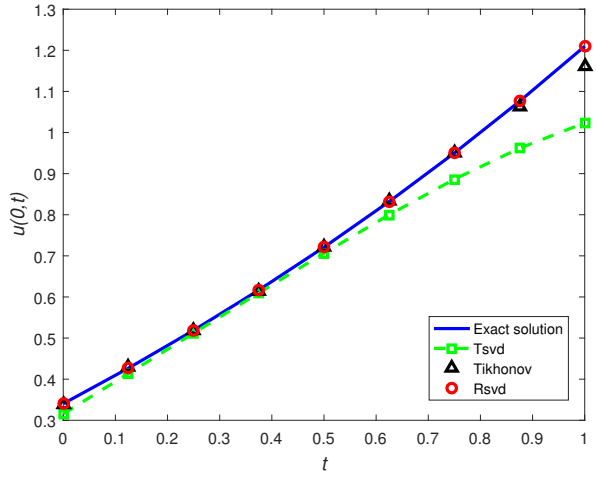

Fig. 7. The comparison of the exact solution and the MFS approximation using three methods generated by l=2.5, $\alpha = 10^{-5}$, k=30 and N=16.

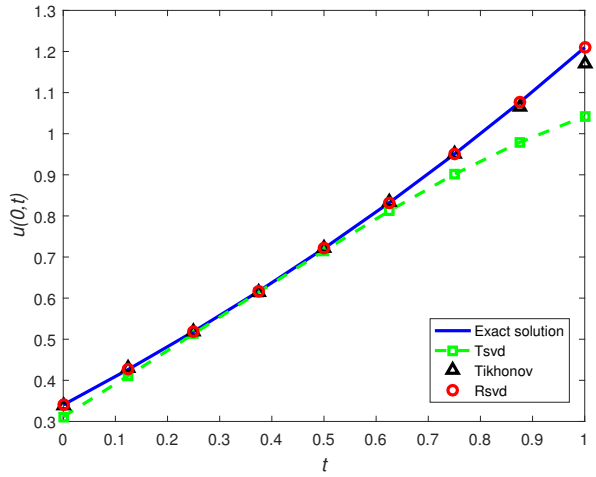

Fig. 8. The comparison of the exact solution and the MFS approximation using three methods generated by l=2.5, $\alpha = 10^{-5}$, k=30 and N=32.

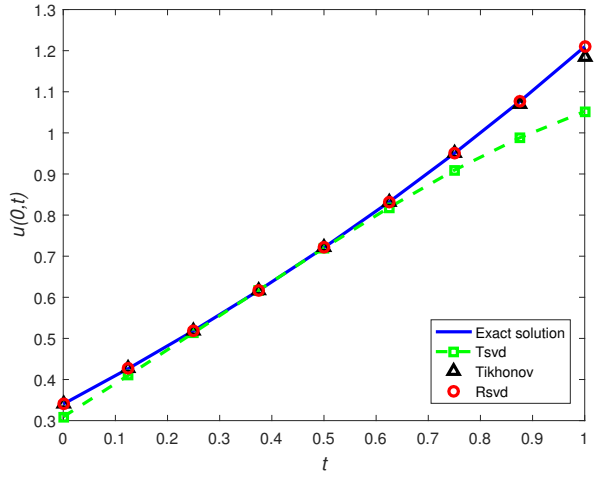

Fig. 9. The comparison of the exact solution and the MFS approximation using three methods generated by l=2.5, $\alpha = 10^{-5}$, k=30 and N=64.

to the TSVD and Tikhonov methods as N increases with α=10^{-6}. Figures 7-10 show that the fundamental solutions

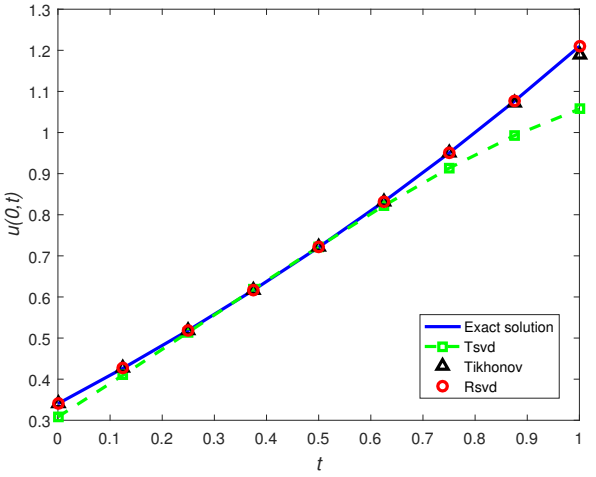

Fig. 10. The comparison of the exact solution and the MFS approximation using three methods generated by l=2.5, $\alpha = 10^{-5}$, k=30 and N=128.

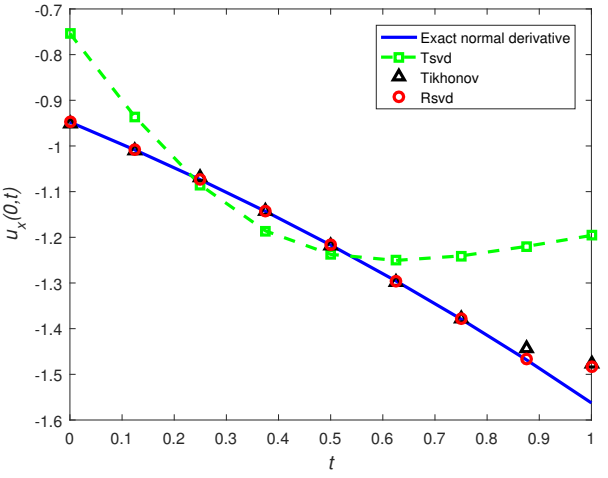

Fig. 11. The comparison of the exact normal derivative and the MFS approximation using three methods generated by l=2.5, $\alpha = 10^{-6}$, k=30 and N=16.

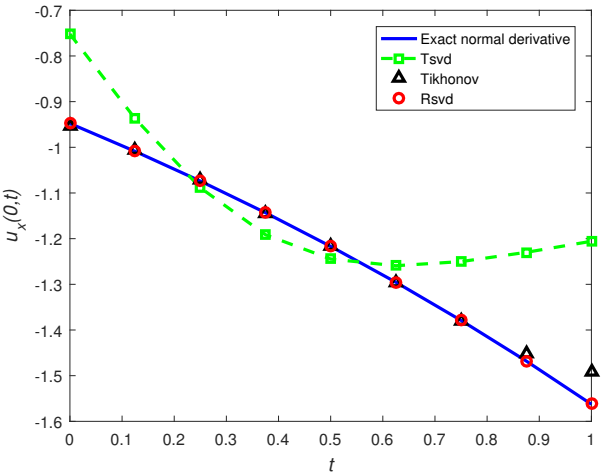

Fig. 12. The comparison of the exact normal derivative and the MFS approximation using three methods generated by l=2.5, $\alpha = 10^{-6}$, k=30 and N=32.

method with the rSVD regularization method is stable and

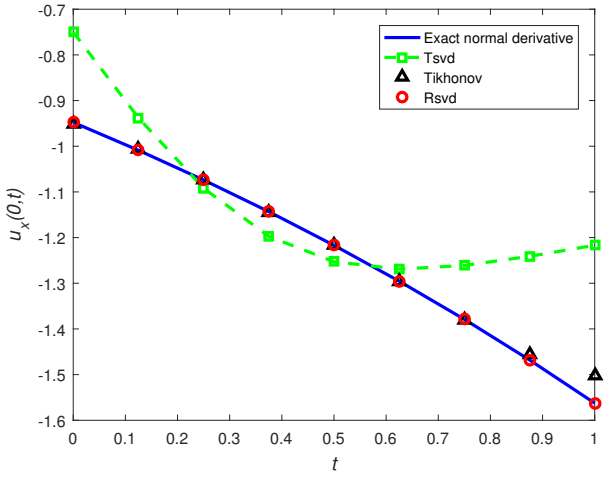

Fig. 13. The comparison of the exact normal derivative and the MFS approximation using three methods generated by l=2.5, $\alpha = 10^{-6}$, k=30 and N=64.

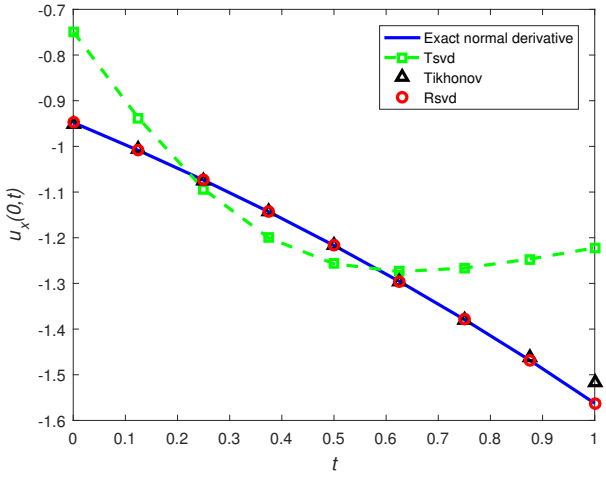

Fig. 14. The comparison of the exact normal derivative and the MFS approximation using three methods generated by l=2.5, $\alpha = 10^{-6}$, k=30 and N=128.

TABLE II
THE COMPARISON OF THE ERROR BETWEEN TSVD, TIKHONOV, RSVD AND THE EXACT SOLUTION FOR DIFFERENT VALUES OF THE SOURCE POINTS N.

boundary	α	N	TSVD	Tikhonov	rSVD
Dirichlet	10^{-6}	16	0.1864	0.0264	0.0180
Dirichlet	10^{-6}	32	0.1675	0.0206	2.1734e-04
Dirichlet	10^{-6}	64	0.1576	0.0168	1.2468e-05
Dirichlet	10^{-6}	128	0.1526	0.0118	3.0710e-06
Dirichlet	10^{-5}	16	0.1864	0.0484	0.0181
Dirichlet	10^{-5}	32	0.1675	0.0392	2.1734e-04
Dirichlet	10^{-5}	64	0.1576	0.0260	1.2264e-05
Dirichlet	10^{-5}	128	0.1526	0.0208	2.5160e-06
Neumann	10^{-6}	16	0.3781	0.0858	0.0784
Neumann	10^{-6}	32	0.3568	0.0710	0.0014
Neumann	10^{-6}	64	0.3458	0.0599	1.0679e-04
Neumann	10^{-6}	128	0.3402	0.0447	3.5315e-05

becomes more accurate when the regularization parameter is changed α=10^{-5}.

The results in Table 2 are consistent with the previous conclusions, indicating that the approximation of the Method of Fundamental Solutions with rSVD regularization becomes more accurate as the number of source points N along x=0 increases, compared to both the TSVD and Tikhonov regularization methods. Consequently, we can conclude that accurate and stable results can be achieved with a high number of source points.

Additionally, we compared the computation time of these methods to demonstrate the efficiency of our proposed approach. The Tikhonov method takes 2.3125s, the TSVD method takes 2.6406s, while the proposed rSVD method only takes 2.2344s. The rSVD method exhibits significant superiority in terms of computation time. Experimental data further confirm that the method proposed in this paper reduces the computational time effectively with l=2.5, α=10^{-6}, and N=128.

In this example, we achieved accurate results with absolute errors of 10^{-6}, which was expected given that the error in the Neumann boundary condition was 10^{-5}.

Our numerical results are comparable to those previously obtained in [2] using the fundamental solutions method with Tikhonov regularization.

In the first example, we utilized a linear moving boundary function M(t). In the subsequent example, we employ a non-linear boundary function.

B. Example 2

The second example features a moving boundary defined by the non-linear function [25].

$$M(t) = 2 - \sqrt{3-2t}, t \in [0,1] \tag{24}$$

The source points are located on the external boundaries $(-l,\mu), \mu \in (-1,1), (M(\mu)+l,\mu), \mu \in (0,1), (M(-\mu)+l,\mu), \mu \in (-1,0)$.

The exact solution is given by

$$v(x,t) = -\frac{x^2}{2} + 2x - \frac{1}{2} - t, (x,t) \in [0, M(t)] \times [0,1] \tag{25}$$

Such as this example has the following initial and boundary conditions

$$v(x,0) = -\frac{x^2}{2} + 2x - \frac{1}{2}, x \in [0, M(0)], M(0) = 2 - \sqrt{3} \tag{26}$$

$$v(M(t),t) = 0, t \in (0,1] \tag{27}$$

$$\frac{\partial v}{\partial x}(M(t),t) = -M^{'}(t) = \sqrt{3-2t}, t \in (0,1] \tag{28}$$

The Dirichlet and Neumann boundary conditions on the fixed boundary x=0 is given by

$$v(0,t) = -\frac{1}{2} - t, t \in [0,1] \tag{29}$$

$$\frac{\partial v}{\partial x}(0,t) = 2, t \in [0,1] \tag{30}$$

We have demonstrated the MFS approximations in Figures 15-18 and Figures 19-22 to determine the Dirichlet condition using three different types of regularization with α=10^{-6} and α=10^{-5}. Our findings indicate that the rSVD regularization achieves greater accuracy as the number of source

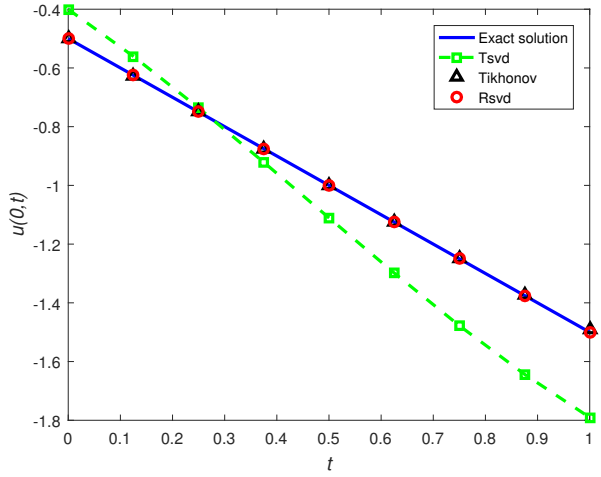

Fig. 15. The comparison of the exact solution and the MFS approximation using three methods generated by l=2.5, $\alpha = 10^{-6}$, k=30 and N=16.

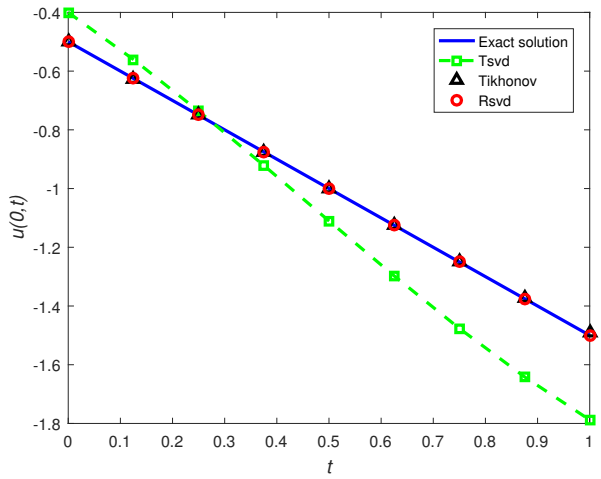

Fig. 16. The comparison of the exact solution and the MFS approximation using three methods generated by l=2.5, $\alpha = 10^{-6}$, k=30 and N=32.

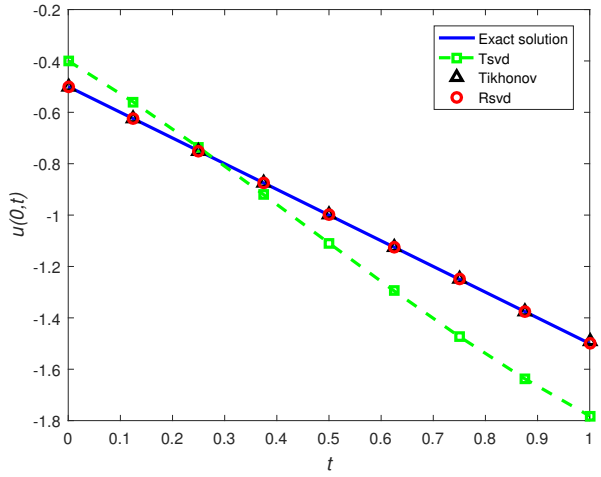

Fig. 17. The comparison of the exact solution and the MFS approximation using three methods generated by l=2.5, $\alpha = 10^{-6}$, k=30 and N=64.

points increases when compared to the TSVD and Tikhonov regularization methods, as previously reported in [2].

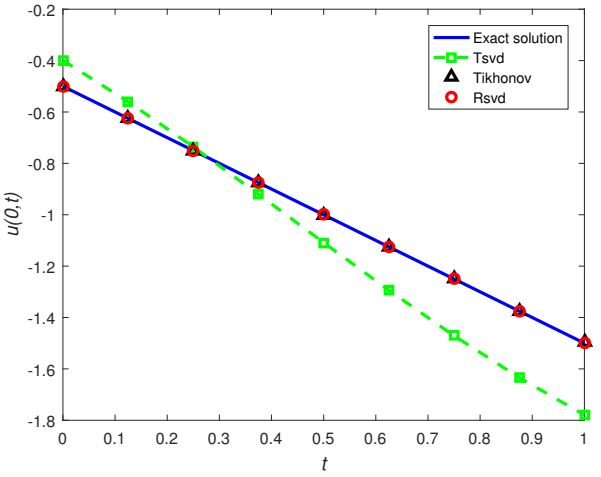

Fig. 18. The comparison of the exact solution and the MFS approximation using three methods generated by l=2.5, $\alpha = 10^{-6}$, k=30 and N=128.

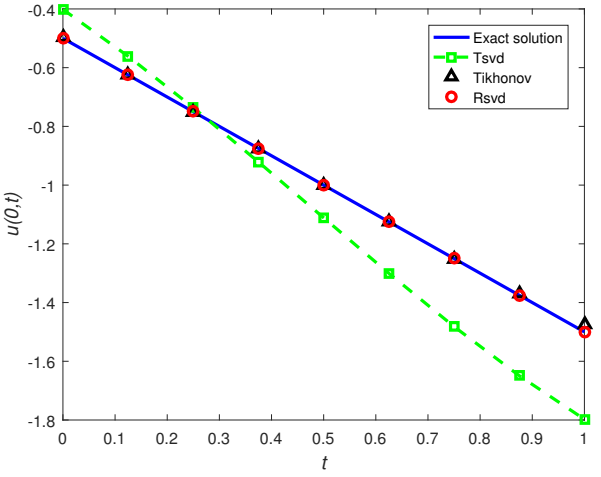

Fig. 19. The comparison of the exact solution and the MFS approximation using three methods generated by l=2.5, $\alpha = 10^{-5}$, k=30 and N=16.

A comparison of the computation time for these methods when applied to the second example reveals the efficiency of our proposed approach. The Tikhonov method takes 3.625s, the TSVD method takes 2.9375s, while the proposed rSVD method only takes 2.7813s. The rSVD method exhibits significant superiority in terms of computation time. Experimental data further confirm that our proposed method reduces the computational time effectively with l=2.5, α=10^{-6}, and N=128. The Neumann boundary conditions on the fixed boundary x=0 are presented in Figures 23-26. These figures depict the exact solution and the MFS approximation for the normal derivative v_x(0,t) using three types of regularization. Similar to Example 1, the rSVD regularization appears to become more accurate as N increases, compared to the Tikhonov regularization [2]. However, the TSVD approximation exhibits slightly oscillatory and unstable behavior, supporting the conclusion that our method is more accurate.

The Neumann boundary conditions on the fixed boundary x=0 is presented in Figures 23-26.

From Table 3, we can deduce that the rSVD method outperforms the TSVD and Tikhonov methods when the regularization parameter is set to α=10^{-5} and α=10^{-6}. In

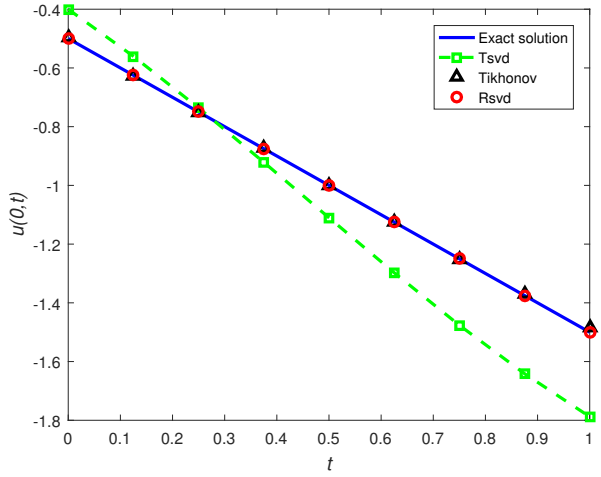

Fig. 20. The comparison of the exact solution and the MFS approximation using three methods generated by l=2.5, $\alpha = 10^{-5}$, k=30 and N=32.

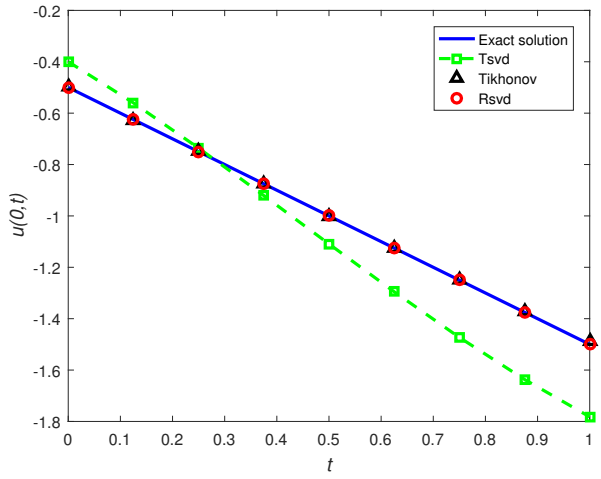

Fig. 21. The comparison of the exact solution and the MFS approximation using three methods generated by l=2.5, $\alpha = 10^{-5}$, k=30 and N=64.

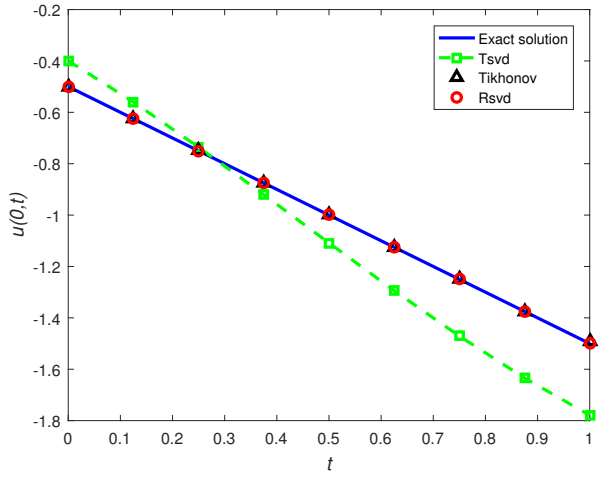

Fig. 22. The comparison of the exact solution and the MFS approximation using three methods generated by l=2.5, $\alpha = 10^{-5}$, k=30 and N=128.

both examples 1 and 2, we increase the number of source points to investigate their impact on the results. We set

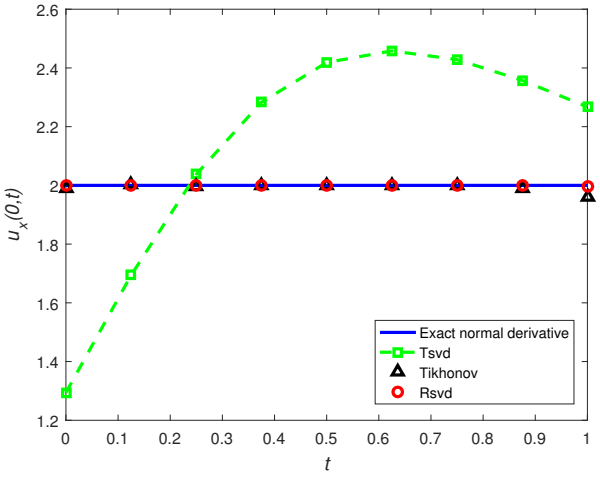

Fig. 23. The comparison of the exact normal derivative and the MFS approximation using three methods generated by l=2.5, $\alpha = 10^{-6}$, k=30 and N=16.

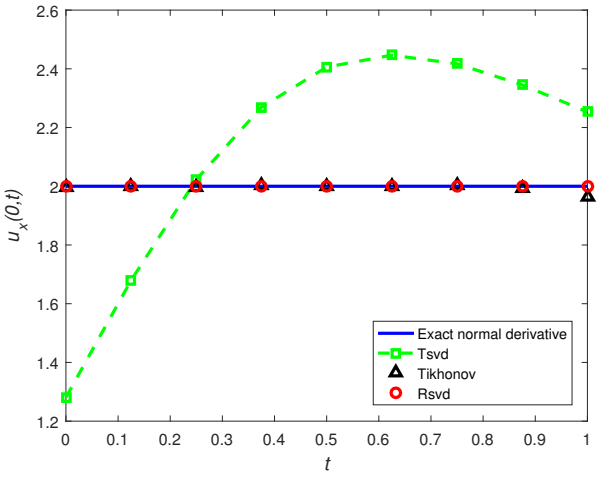

Fig. 24. The comparison of the exact normal derivative and the MFS approximation using three methods generated by l=2.5, $\alpha = 10^{-6}$, k=30 and N=32.

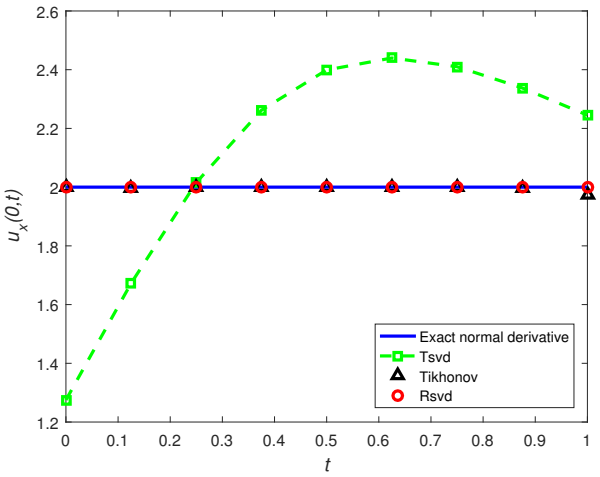

Fig. 25. The comparison of the exact normal derivative and the MFS approximation using three methods generated by l=2.5, $\alpha = 10^{-6}$, k=30 and N=64.

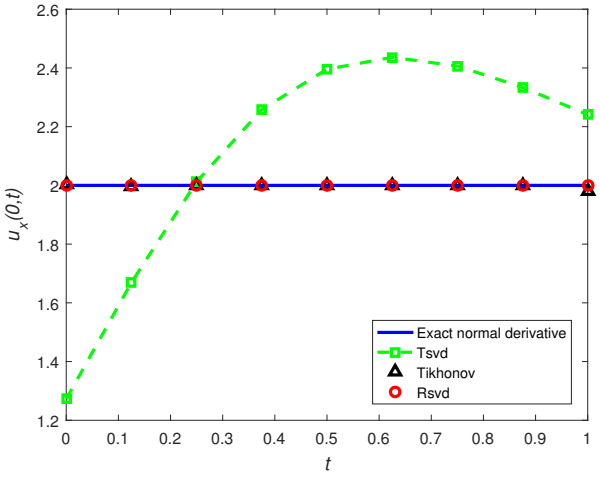

Fig. 26. The comparison of the exact normal derivative and the MFS approximation using three methods generated by l=2.5, $\alpha = 10^{-6}$, k=30 and N=128.

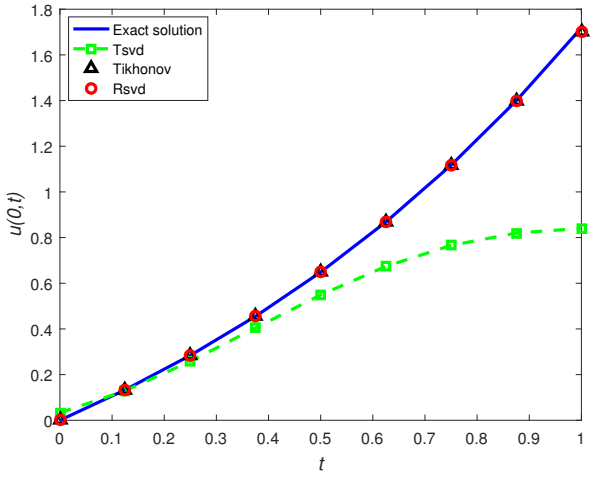

Fig. 27. The comparison of the exact solution and the MFS approximation using three methods generated by l=1.7, $\alpha = 10^{-13}$, k=30 and N=16.

TABLE III
THE COMPARISON OF THE ERROR BETWEEN TSVD, TIKHONOV, RSVD AND THE EXACT SOLUTION FOR DIFFERENT VALUES OF THE SOURCE POINTS N.

boundary	α	N	TSVD	Tikhonov	rSVD
Dirichlet	10^{-6}	16	0.2976	0.0111	0.0033
Dirichlet	10^{-6}	32	0.0097	0.0096	1.4823e-04
Dirichlet	10^{-6}	64	0.2822	0.0066	8.3041e-06
Dirichlet	10^{-6}	128	0.2791	0.0049	4.2907e-07
Dirichlet	10^{-5}	16	0.2976	0.0239	0.0031
Dirichlet	10^{-5}	32	0.2879	0.0172	1.4822e-04
Dirichlet	10^{-5}	64	0.2822	0.0112	7.0089e-06
Dirichlet	10^{-5}	128	0.2791	0.0096	6.7863e-07
Neumann	10^{-6}	16	0.7059	0.0385	0.0041
Neumann	10^{-6}	32	0.7189	0.0350	4.6159e-04
Neumann	10^{-6}	64	0.7249	0.0249	6.2810e-05
Neumann	10^{-6}	128	0.7279	0.0198	2.8883e-06

N to $\{16, 32, 64, 128\}$ and observe that these results were generated using the TSVD, Tikhonov, and rSVD methods.

The numerical results demonstrate that increasing the number of source points (N) significantly enhances the accuracy of the outcomes, with the rSVD method being more accurate than the Tikhonov and TSVD methods. Consequently, we can confidently conclude that accurate and stable results can be achieved with a relatively high number of source points.

C. Example 3

In this example, the function defines a moving boundary as follows:

$$M(t) = t, t \in [0, 1] \tag{31}$$

The source points are located on the external boundaries.

$(-l, \mu), \mu \in (-1, 1), (M(\mu)+l, \mu), \mu \in (0, 1), (M(-\mu)+l, \mu), \mu \in (-1, 0)$.

The exact solution is given by

$$v(x, t) = -1 + exp(t - x), (x, t) \in [0, 1] \times [0, 1] \tag{32}$$

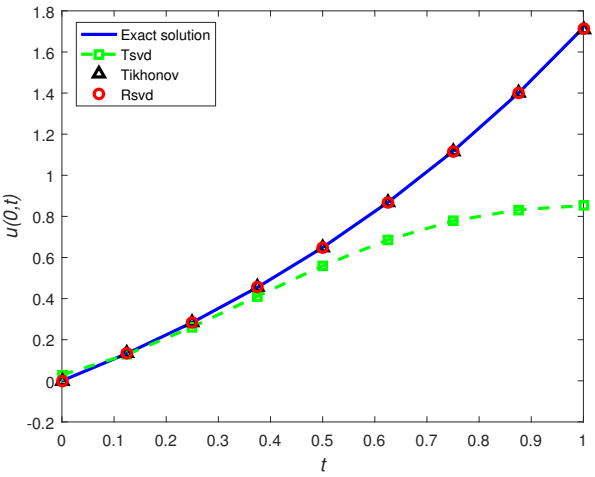

Fig. 28. The comparison of the exact solution and the MFS approximation using three methods generated by l=1.7, $\alpha = 10^{-13}$, k=30 and N=32.

In the present example, the initial and boundary conditions are as follows:

$$v(x, 0) = -1 + exp(t), x \in [0, M(0)], M(0) = 0 \tag{33}$$

$$v(M(t), t) = 0, t \in (0, 1] \tag{34}$$

$$\frac{\partial v}{\partial x}(M(t), t) = -M^{'}(t) = -1, t \in (0, 1] \tag{35}$$

The Dirichlet and Neumann boundary conditions on the fixed boundary x=0 is given by

$$v(0, t) = -1 + exp(t), t \in [0, 1] \tag{36}$$

$$\frac{\partial v}{\partial x}(0, t) = -exp(t), t \in [0, 1] \tag{37}$$

Figures 27-30 depict the MFS approximations employed for determining the Dirichlet condition, utilizing three distinct types of regularization with α=10^{-13}. When compared to the TSVD and Tikhonov regularization methods, our findings demonstrate that the rSVD regularization approach achieves enhanced accuracy as the number of source points increases. Neumann boundary conditions on the fixed boundary x=0 are presented in Figures 31-34.

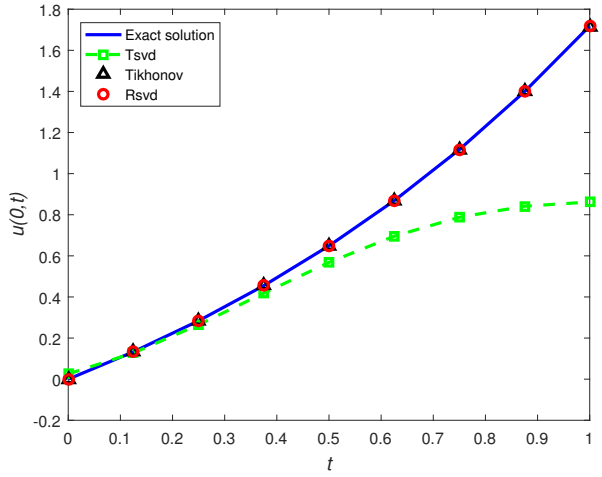

Fig. 29. The comparison of the exact solution and the MFS approximation using three methods generated by l=1.7, $\alpha = 10^{-13}$, k=30 and N=64.

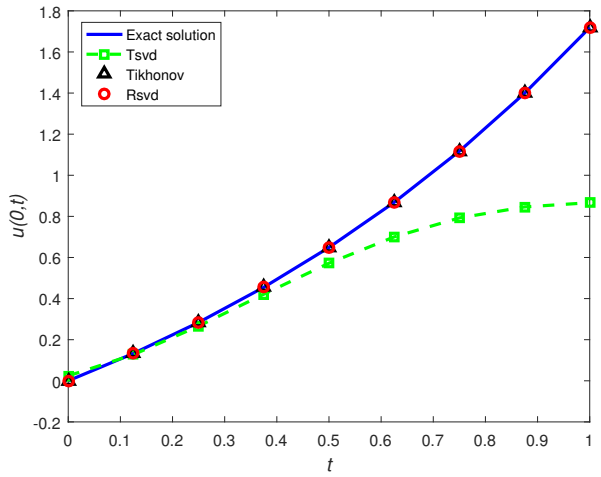

Fig. 30. The comparison of the exact solution and the MFS approximation using three methods generated by l=1.7, $\alpha = 10^{-13}$, k=30 and N=128.

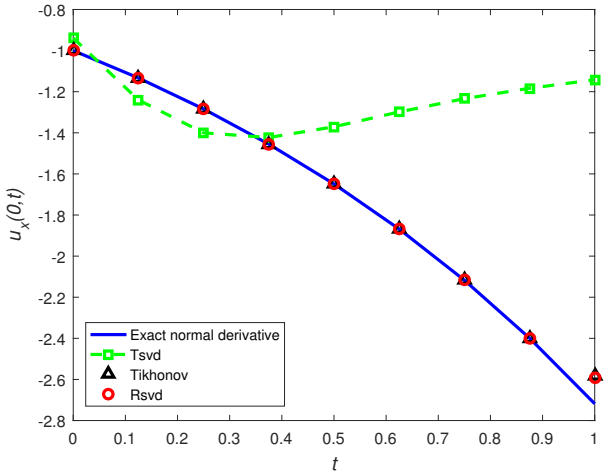

Fig. 31. The comparison of the exact normal derivative and the MFS approximation using three methods generated by l=1.7, $\alpha = 10^{-13}$, k=30 and N=16.

Figures 31-34 illustrate the Neumann boundary conditions on the fixed boundary x=0. These graphs depict both the

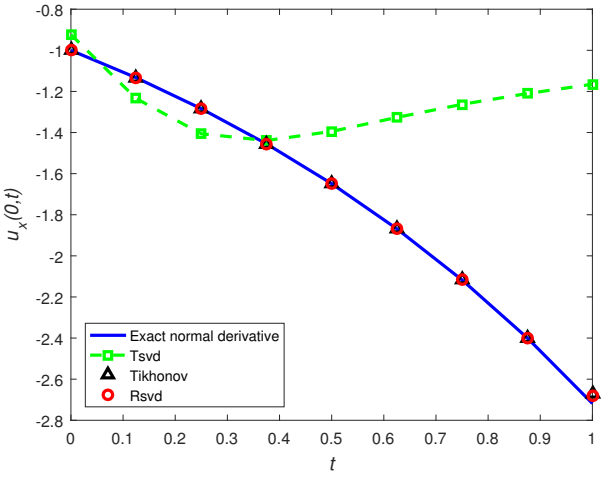

Fig. 32. The comparison of the exact normal derivative and the MFS approximation using three methods generated by l=1.7, $\alpha = 10^{-13}$, k=30 and N=32.

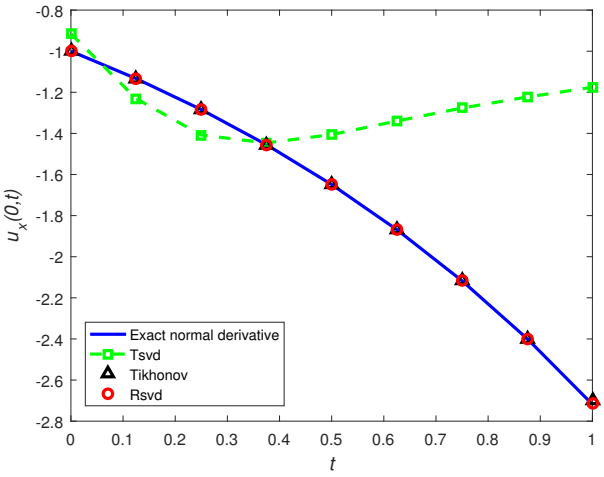

Fig. 33. The comparison of the exact normal derivative and the MFS approximation using three methods generated by l=1.7, $\alpha = 10^{-13}$, k=30 and N=64.

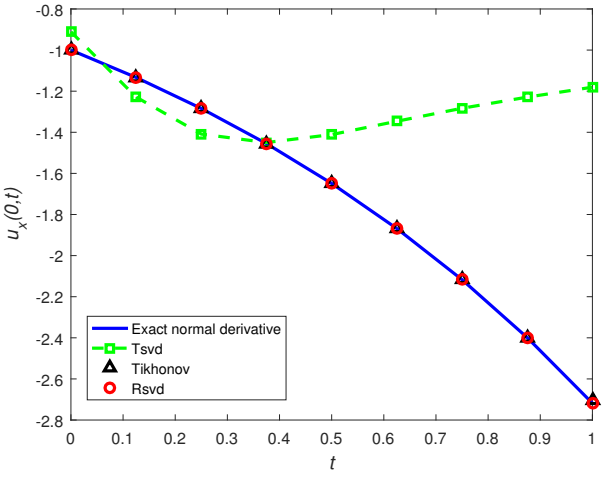

Fig. 34. The comparison of the exact normal derivative and the MFS approximation using three methods generated by l=1.7, $\alpha = 10^{-13}$, k=30 and N=128.

TABLE IV
THE COMPARISON OF THE ERROR BETWEEN TSVD, TIKHONOV, RSVD AND THE EXACT SOLUTION FOR DIFFERENT VALUES OF THE SOURCE POINTS N.

boundary	α	N	TSVD	Tikhonov	rSVD
Dirichlet	10^{-13}	16	0.8864	0.0286	0.0276
Dirichlet	10^{-13}	32	0.8657	0.0073	0.0057
Dirichlet	10^{-13}	64	0.8562	0.0026	7.6305e-04
Dirichlet	10^{-13}	128	0.8517	0.0016	9.5944e-05
Neumann	10^{-13}	16	1.5763	0.1378	0.1357
Neumann	10^{-13}	32	1.5532	0.0445	0.032
Neumann	10^{-13}	64	1.5427	0.0186	0.0064
Neumann	10^{-13}	128	1.5376	0.0122	9.8830e-04

exact solution and the MFS approximation for the normal derivative v_x(0,t) using three different forms of regularization. When compared to Tikhonov regularization, the rSVD regularization appears to be more accurate as N grows. In contrast, the TSVD approximation exhibits slightly oscillatory and unstable behavior, reinforcing our conclusion that our method is more accurate.

The results in Table 4 indicate that the Method of Fundamental Solutions approximation with rSVD regularization becomes more accurate as the number of source points (N) along x=0 increases, in comparison to both the TSVD and Tikhonov regularization methods. Consequently, we can conclude that accurate and consistent results are attainable.

VI. CONCLUSION

In this paper, we introduced the fundamental solutions method for determining the Dirichlet and Neumann conditions of the one-dimensional inverse Stefan problem, employing different types of regularization. Our findings indicate that utilizing the MFS with rSVD regularization yields more accurate results compared to TSVD and Tikhonov regularization.

The numerical examples demonstrate the accuracy of the MFS in determining boundary data for inverse Stefan problems. In our future work, we plan to investigate the accuracy and effectiveness of this method for other classes of problems, including direct problems and the two-dimensional inverse Stefan problem.

REFERENCES

[1] L. I. Rubinstein, "The Stefan problem," Translations of Mathematical Monographs, Vol. 27, pp94-135, 1971

[2] B. Tomas Johansson, D. Lesnic, and T. Reeve, "A method of fundamental solutions for the one-dimensional inverse Stefan problem," Applied Mathematical Modelling, vol. 35, no.9, pp4367-4378, 2011

[3] B. Tomas Johansson, Daniel Lesnic, and Thomas Reeve, "The method of fundamental solutions for the two-dimensional inverse Stefan problem," Inverse Problems in Science and Engineering, vol. 22, no.1, pp112-129, 2014

[4] Sergio Andrés Ardila-Parra, Carmine Maria Pappalardo, Octavio Andrés González Estrada, and Domenico Guida, "Finite Element based Redesign and Optimization of Aircraft Structural Components using Composite Materials," IAENG International Journal of Applied Mathematics, vol. 50, no.4, pp860–877, 2020

[5] Kanokwan Pananu, Surattana Sungnul, Sekson Sirisubtawee and Sutthisak Phongthanapanich, "Convergence and Applications of the Implicit Finite Difference Method for Advection-Diffusion-Reaction Equations," IAENG International Journal of Computer Science, vol. 47, no.4, pp645-663, 2020

[6] Supranee Chonladed, and Kanognudge Wuttanachamsri, "A Numerical Solution of Burger's Equation Based on Milne Method," IAENG International Journal of Applied Mathematics, vol. 51, no.2, pp411-415, 2021

[7] Erny Rahayu Wijayanti, Sumardi, and Nanang Susyanto, "European Call Options Pricing Numerically using Finite Element Method," IAENG International Journal of Applied Mathematics, vol. 52, no.4, pp940-945, 2022

[8] S. Chantasiriwan, B.Tomas Johansson, and D. Lesnic, "The method of fundamental solutions for free surface problem," Engineering Analysis with Boundary Elements, vol. 33, no.4, pp529-538, 2009

[9] B. Tomas Johanssona, Daniel Lesnic, and Thomas Reeve, "The method of fundamental solutions for the two-dimensional inverse Stefan problem," Inverse Problems in Science and Engineering, vol. 22, no.1, pp112–129, 2014

[10] M. Gu, "Subspace iteration randomization and singular value problems," SIAM Journal on Scientific Computing, vol. 37, no.3, ppA1139-A1173, 2015

[11] Rafi Witten and Emmanuel Candès, "Randomized algorithms for low-rank matrix factorizations: sharp performance bounds," Algorithmica, vol. 72, no.1, pp264-281, 2015

[12] J. R. Cannon and C. Denson Hill, "Existence, uniqueness, stability, and monotone dependence in a Stefan problem for the heat equation," Journal of Mathematics and Mechanics, vol. 17, no.1, pp1-19, 1967

[13] N. L. Gol'dman, "Inverse Stefan Problem," Kluwer Academic Publishers, 1997

[14] B. Tomas Johansson, and Daniel Lesnic, "A method of fundamental solutions for transient heat conduction," Engineering Analysis with Boundary Elements, vol. 32, no.9, pp697-703, 2008

[15] B. Tomas Johansson, and Daniel Lesnic, "A method of fundamental solutions for transient heat conduction in layered materials," Engineering Analysis with Boundary Elements, vol. 33, no.12, pp1362-1367, 2009

[16] C.S. Chen, Hokwon A. Cho, M. A. Golberg, "Some comments on the ill-conditioning of the method of fundamental solutions," Engineering Analysis with Boundary Elements, vol. 30, no.5, pp405-410, 2006

[17] P. A. Ramachandran, "Method of fundamental solutions: singular value decomposition analysis," Communications in Numerical Methods in Engineering, vol. 18, no.11, pp789-801, 2002

[18] Jingjing Cui, Guohua Peng, Quan Lu, and Zhengge Huang, "Special Regularized HSS Iteration Method for Tikhonov Regularization," IAENG International Journal of Applied Mathematics, vol. 50, no.2, pp359-372, 2020

[19] Per Christian Hansen, "Analysis of discrete ill-posed problems by means of the L-curve," Society for Industrial and Applied Mathematics, vol. 34, no.4, p561-580, 1992

[20] Per Christian Hansen, "The truncated SVD as a method for regularization," BIT Numerical Mathematics, vol. 27,no.4 pp534–553, 1987

[21] Kazufumi Ito and Bangti Jin, "Regularized Linear Inversion with Randomized Singular Value Decomposition," Mathematical and Numerical Approaches for Multi-Wave Inverse Problems, vol. 328, pp45–72, 2019

[22] Xingyu Tuo, Yin Zhang, Yingying Wang, Deqing Mao, Yongchao Zhang, and Yulin Huang, "A Fast Angle Super-resolution Imaging Method for Airborne Scanning Radar based on rSVD," 2019 International Radar Conference (RADAR), pp1-5, 2019

[23] Jean-Luc Chabert, "Gauss et la méthode des moindres carrés," Revue d'histoire des sciences, vol. 42, no.1, pp5-26, 1989

[24] Diego A. Murio, "Solution of inverse heat conduction problems with phase changes by the mollification method," Computers and Mathematics with Applications, vol. 24, no.7, pp45-57, 1992

[25] G. M. M. Reddy, M. Vynnycky, and J. A. Cuminato, "On efficient reconstruction of boundary data with optimal placement of the source points in the MFS: application to inverse Stefan problems," Inverse Problems in Science and Engineering, vol. 26, no.9, pp1741-5977, 2017